AGU PUBLICATIONS

Water Resources Research

RESEARCH ARTICLE
10.1002/2016WR018933

Special Section:
Modeling highly heterogeneous aquifers: Lessons learned in the last 30 years from the MADE experiments and others

Aquifer heterogeneity controls on adverse human health effects and the concept of the hazard attenuation factor

F. P. J. de Barros[1], A. Bellin[2], V. Cvetkovic[3], G. Dagan[4], and A. Fiori[5]

[1]Sonny Astani Department of Civil and Environmental Engineering, University of Southern California, Los Angeles, California, USA, [2]Department of Civil, Environmental and Mechanical Engineering, University of Trento, Trento, Italy, [3]Division of Water Resources Engineering, KTH Royal Institute of Technology, Stockholm, Sweden, [4]School of Mechanical Engineering, Tel Aviv University, Ramat Aviv, Israel, [5]Dipartimento di Ingegneria, Universita' di Roma Tre, Rome, Italy

Key Points:
- Aquifer heterogeneity controls the PDF of risk
- Introduction of the concept of hazard attenuation factor
- Hazard attenuation factor PDF for various levels of heterogeneity

Correspondence to:
F. P. J. de Barros,
fbarros@usc.edu

Citation:
de Barros, F. P. J., A. Bellin, V. Cvetkovic, G. Dagan, and A. Fiori (2016), Aquifer heterogeneity controls on adverse human health effects and the concept of the hazard attenuation factor, *Water Resour. Res.*, *52*, 5911–5922, doi:10.1002/2016WR018933.

Received 14 MAR 2016
Accepted 13 JUL 2016
Accepted article online 18 JUL 2016
Published online 6 AUG 2016

Abstract We analyze the probability distribution of the hazard attenuation factor for a noncarcinogenic reactive compound captured by a well in heterogeneous porous formations. The hazard attenuation factor is defined as the ratio between the hazard index HI at a detection well and at the source. Heterogeneity of the aquifer is represented through the multi-indicator model (a collection of blocks of independent permeability) while flow and transport are solved by the means of the self-consistent approach that is able to deal with any degree of heterogeneity. Due to formation heterogeneity, HI is a random variable and similar for hazard attenuation index. The latter can be fully characterized by its cumulative distribution function (CDF), which in turn can be related to the statistics of the travel time of solute particles, from the source to the detection well. The approach is applied to the case of a solute which undergoes decay and a well with a screen much smaller than the correlation scale of hydraulic conductivity. The results show that the probability of exceeding a given acceptable threshold of the hazard index is significantly affected by the level of heterogeneity comparable to the one observed for the MADE site, and the distance between the source and the well.

1. Introduction

Assessing human exposure to contaminated groundwater is a major challenge in many parts of the world. Defining contaminant mass fluxes in natural porous media is an arduous task since scientists and engineers need to cope with multiscale spatial variability of hydrogeological properties. Capturing the spatial patterns of the subsurface's hydraulic parameters, such as the permeability, is a key component in the prediction of large-scale transport behavior [*Dagan*, 1989; *Rubin*, 2003] and consequently, in risk assessment [*Rubin et al*., 1994; *de Barros and Fiori*, 2014]. Due to limited financial resources and technical difficulties, a full characterization of geological formation is not feasible. Scarce site characterization data causes uncertainty in flow and contaminant transport predictions, and therefore the human exposure to contaminants and the associated adverse health effects must be treated in a probabilistic manner [e.g., *Maxwell and Kastenberg*, 1999]. Hence, reliable human health risk estimation requires improved assessment of the impact of the spatial patterns of variability of the geological hydraulic properties onto transport and exposure models. Aside from the geological formation, other sources of uncertainty include source strength and its location, as well as uncertainty about attenuation and transformation reactions, human physiological response, and behavioral characteristics [e.g., *Bogen and Spear*, 1987; *Maxwell and Kastenberg*, 1999; *de Barros and Rubin*, 2008; *Andricevic et al*., 2012].

There is a large number of works dedicated to addressing human health risk utilizing probabilistic and geostatistics tools for distinct pollutants such as chlorinated solvents [*Maxwell and Kastenberg*, 1999; *Benekos et al*., 2007; *Henri et al*., 2015, 2016], pathogens [*Molin and Cvetkovic*, 2010; *Cvetkovic and Molin*, 2012], by-products of CO_2 leakage [*Siirila et al*., 2012; *Atchley et al*., 2013], arsenic [*Yu et al*., 2003], cadmium leaching [*Beyer et al*., 2009], and radioactive waste [*Andrivevic et al*., 1994; *Andricevic and Cvetkovic*, 1996]. Task-oriented human health risk driven approaches have been developed to assist decision makers to best allocate subsurface site characterization resources toward uncertainty reduction in model predictions [*Maxwell et al*., 1999; *de Barros and Rubin*, 2008; *de Barros et al*., 2009, 2012]. The impact of hydraulic conductivity spatial heterogeneity on the stochastic characterization of human health risk and related metrics are also

reported in the literature [*de Barros and Fiori*, 2014; *Fiori et al*., 2015a]. *Henri et al*. [2016] focused on the effects of DNAPL source release conditions in heterogeneous aquifers on the overall statistical characterization of the increased lifetime cancer risk. Most of these works are focused on geological formations displaying low-to-mild heterogeneity where analytical solutions were derived for the ensemble moments of the increased lifetime cancer risk [*Andricevic and Cvetkovic*, 1996; *de Barros and Rubin*, 2008; *de Barros and Fiori*, 2014] and microbial infection [*Molin and Cvetkovic*, 2010; *Molin et al*., 2010]. The significance of statistical anisotropy of the permeability field in controlling carcinogenic and noncarcinogenic health effects was shown analytically for nonreactive contaminants [*de Barros and Fiori*, 2014] and numerically for reactive transport [*Siirila and Maxwell*, 2012]. *Rodak and Silliman* [2012] used a fault tree framework [see *Tartakovsky*, 2007] to study risks to human health for improved wellhead protection and managing groundwater resources. *Tartakovsky* [2013] provides a review of different methodologies for propagation of uncertainty in probabilistic risk analysis applications in hydrology.

Despite the significant progress there are still research needs to improve our fundamental understanding of how spatial heterogeneity of the hydraulic properties affect the statistical description of solute concentration and health risk. As discussed in the AGU Chapman Conference, held in Valencia (Spain) in October 2015 [*Gomez-Hernandez et al*., 2016], aquifer heterogeneity is one of the key factors hampering our ability to successfully remediate the subsurface environment. Thus, in contrast to most aforementioned studies dealing with weak to moderate heterogeneous aquifers, in the present work we address the effect of strong heterogeneity on health risk assessment. This is the case of the MADE site [*Harvey and Gorelick*, 2000; *Zheng et al*., 2011; *Bohling et al*., 2012], but also of many other aquifers, as set forth at the recent Chapman conference [*Gomez-Hernandez et al*., 2016]. Toward this aim, we employ the recently developed physically based model of flow and transport coined as MIMSCA (*Multi-Indicator Model* of aquifer structure and *Self Consistent Approximation* of flow and transport) [e.g., *Cvetkovic et al*., 2014], which was shown to predict the observed plume snapshots [*Fiori et al*., 2013] at the MADE experiment. MIMSCA revealed a few specific features of the breakthrough curves in transport through highly heterogeneous media, e.g., a long tailing caused by contaminant retention in zones of low permeability on one hand and presence of channels of fast solute advance on the other [e.g., *Salamon et al*., 2007; *Fiori and Jankovic*, 2012; *Fiori et al*., 2013; *Dogan et al*., 2014; *Fiori et al*., 2015b].

The plan of the paper is as follows. The problem formulation is stated in section 2. Details pertaining the methodological approach are given in section 3. Section 4 provides results and conclusions are given in section 5.

2. Problem Statement

2.1. General Background

We consider a steady state flow field within an aquifer of a spatially heterogeneous hydraulic conductivity field $K(\mathbf{x})$, with $\mathbf{x}=(x,y,z)$ representing the Cartesian coordinate system. The hydraulic conductivity, or its log-conductivity $Y(\mathbf{x})=\ln[K(\mathbf{x})]$, is modeled as a stationary random space function (RSF) [*Dagan*, 1989; *Rubin*, 2003]. Thus, the RSF is characterized by the univariate probability density function (PDF) of mean $\langle Y\rangle=\ln K_G$ (with K_G the geometric mean), variance σ_Y^2 and axisymmetric two point covariance $C_Y(r)=\sigma_Y^2\rho_Y(\mathbf{r})$, where $\mathbf{r}$ is the lag distance. The autocorrelation $\rho_Y(\mathbf{r})$ is characterized by the horizontal integral scale I (i.e., $x-y$ plane) and the vertical integral scale I_v (i.e., direction z). In this work, the angle brackets $\langle\cdot\rangle$ represent ensemble averaging.

As a consequence of the heterogeneity of $K(\mathbf{x})$, the steady state Darcy-scale velocity field $\mathbf{V}(\mathbf{x})$ is spatially variable and random. The equations of flow and continuity are

$$\mathbf{V}(\mathbf{x})=-\frac{K(\mathbf{x})}{\phi}\nabla h(\mathbf{x}),\quad \nabla\cdot\mathbf{V}(\mathbf{x})=0, \tag{1}$$

where h is the hydraulic head and ϕ is the effective porosity (assumed to be constant). For the sake of simplicity, we assume that the steady flow field is uniform-in-the-mean such that $\langle\mathbf{V}(\mathbf{x})\rangle=(U,0,0)$. This corresponds to a natural gradient flow, driven by a constant mean head gradient $\langle\nabla h\rangle=(-J,0,0)$, with $U=K_{ef}J/\phi$, where K_{ef} is the effective conductivity.

Water is pumped out at a constant given discharge Q_w by a well (or battery of wells) located in a vertical control plane (CP), at a longitudinal distance x from the contaminant injection plane (IP) located at $x=0$.

Water and solute are drawn by the wells in a capture zone of area $A_w \approx Q_w/U$. With the neglect of the additional spreading caused by the radial flow in a zone adjacent to the well, the average solute concentration at the capture well is given by $C_w(t)=Q_C(x,t)/Q_w$, where $Q_C(x,t)$ is the solute discharge through the area A_w in the CP. The same expression applies for a battery of wells, with Q_w representing the total pumped water discharge. The variable C_w is random due to the dependence of Q_C on the permeability field and it serves as input to health risk assessment, as will be discussed in section 2.2.

A hypothetical toxic reactive solute is assumed to be released continuously at a constant concentration C_0 for a finite duration ΔT, along an areal source A_0 in the injection plane (IP) at $x = 0$. The plume of concentration $C(\mathbf{x},t)$ undergoes decay (e.g., anaerobic biodegradation or radioactive decay), which is modeled by a first order reaction of constant rate λ. In this work, we assume λ to be deterministic however depending on the application, it can be considered to be uncertain.

The aim of the solution of the flow and transport is to derive the random $C_w(t)$ as a function of the various parameters characterizing the problem. A general solution for arbitrary A_0 and A_w is not pursued here, our limited objective being to illustrate the impact of high heterogeneity, i.e., $\sigma_Y^2 > 1$, on risk for a particular configuration. Thus, we assume that the input area A_0 is larger than A_w such that in any realization of the permeability field the well draws contaminated water.

Two extreme cases of the magnitude of the area $A_w < A_0$ are of particular interest. The first one is of $A_w > I\times I_v$, i.e., ergodic injection and capture zones. Then, $Q_C \cong \langle \mu(x,t)\rangle A_w$, where μ is the solute areal flux, i.e., $\langle \mu(x,t)\rangle \cong (1/A_w)\int_{A_w}\phi V_x(x,y,z)C(x,y,z,t)dydz$. In this case $C_w \cong \langle Q_C(x,t)\rangle/Q_w$ is not random, but its magnitude depends on the parameters characterizing the permeability field (e.g., K_G, σ_Y^2, I, and I_v) as well as C_0 and λ. This was the case mostly treated in the literature [e.g., *Cvetkovic et al*., 2014, and references therein].

The second extreme case, to be considered in the present study, is that of $A_w < I\times I_v$, i.e., a small capture zone at the heterogeneity scales, as pertaining to a well of a relatively short screen and of discharge $Q_w \leqslant UII_v$. Then, the concentration in the well is approximately given by

$$C_w|_{t=\tau}=C(\mathbf{x}_w,\tau)=C_0\exp(-\lambda\tau), \tag{2}$$

where C is the local concentration at the point $\mathbf{x}_w=(x,y_w,z_w)$ pertaining to the location of the screen in the CP, while τ is the travel time of the fluid particle traveling from the IP to $\mathbf{x}_w$. Indeed, the well is reached by a streamtube of small cross section originating at a point within the IP and we assume that the effect of dilution and local-scale dispersion can be neglected relative to that of decay, i.e., transport is by advection only. It can be shown that local-scale dispersion has a negligible impact on the local concentration when $\alpha_T U/(I_v^2\lambda) \ll 1$, with α_T the transverse local dispersivity. Any streamtube originating from A_0 is a candidate and τ is a random value linked to the statistics of Y. The computation of τ is carried out in the sequel (section 3) by deriving the random BTC for a resident concentration injection boundary condition at A_0. Thus, the solute discharge at the well is given by Q_wC_w and the total mass captured by the well over a given exposure period of duration ED is given by Q_wC_0EDexp$(-\lambda\tau)$. This extreme case is the one for which the uncertainty of the well solute concentration is the largest and illustrating its impact (as a function of hydrogeological heterogeneity) on health risk is the main objective of this paper.

In the more general case (not considered here) of a capture zone of intermediate size between the extreme cases of $A_w < I\times I_v$ and $A_w \gg I\times I_v$, the uncertainty of C_w is reduced relative to (2) due to the variability of τ and μ over the finite streamtube of area A_w. Summarizing, we focus in analyzing risk and its uncertainty for a well characterized by a small screen intercepting a solute plume traveling in a heterogeneous geological formation. We quantify this uncertainty for various degrees of heterogeneity, manifested through σ_Y^2.

2.2. Adverse Human Health Effects and the Concept of the Hazard Attenuation Factor

With the goal of illustrating the adopted framework and without loss of generality, we will quantify noncarcinogenic health effects through the water ingestion pathway. Details pertaining carcinogenic risks and other risk pathways can be found in *USEPA* [1989]. Noncarcinogenic health effects for a single toxic substance are measured through the dimensionless hazard index [*USEPA*, 1989; *Fjeld et al*., 2007]

$$\mathrm{HI}=\frac{\mathrm{ADD}}{\mathrm{R_fD}}, \tag{3}$$

where ADD is the average daily dose and R_fD is the reference dose. Both ADD and R_fD have units of mg/(kg d). The hazard index provides a quantitative measure of risk for noncarcinogenic effects by comparing the averaged daily intake dose to a reference dose, namely, R_fD. R_fD corresponds to a standard toxicity value inferred from the *no observed adverse effect level* (NOAEL) or the *lowest observed adverse effect level* (LOAEL) obtained through toxicological dose-response studies [*Fjeld et al.*, 2007]. If $HI \geq 1$, there is a possibility that noncarcinogenic health effects may occur. The averaged daily dose for the water intake pathway is given by [*USEPA*, 1989; *Fjeld et al.*, 2007]:

$$\mathrm{ADD} = \frac{\mathrm{IR}}{\mathrm{BW}} \frac{\mathrm{EF}}{\mathrm{AT}} \int_{t_0}^{t_0+ED} C_w(t)dt, \tag{4}$$

where t_0 is the initial time of exposure, ED (year) is the exposure duration period, IR (l/d) is the ingestion rate, BW (kg) is the body weight, AT (day) is the averaged expected lifetime, and EF (d/yr) is the exposure frequency [*USEPA*, 1989]. In this work we assume $t_0 + ED$ to be constant and smaller than the solute release duration ΔT such that C_w is constant. Substituting (2) into (4), equation (3) becomes

$$\mathrm{HI} = \frac{1}{\mathrm{R_fD}} \; C_0 \exp(-\lambda\tau) \; \frac{\mathrm{IR}}{\mathrm{BW}} \frac{\mathrm{EF}}{\mathrm{AT}} \frac{\mathrm{ED}}{} = \mathrm{HI}_0 \exp(-\lambda\tau), \tag{5}$$

where HI_0 is the hazard index pertaining to the source concentration C_0 and equal to $IR \times EF \times ED \times C_0/(BW \times AT \times R_fD)$. Hence, we can define the following ratio:

$$\eta \equiv \frac{\mathrm{HI}}{\mathrm{HI}_0} = \exp(-\lambda\tau), \tag{6}$$

which is an alternative formulation of the tracer attenuation expression introduced by *Cvetkovic* [2011] for a solute undergoing attenuation both in mobile and immobile phases [see *Cvetkovic et al.*, 2014, equation (4)]. The main difference between our work and *Cvetkovic* [2011] is that η is derived in the context of human health risk. Here η is defined as the *hazard attenuation factor*, a random variable characterized by its PDF, which incorporates the combined effect of self-purification (decay) and hydrogeological heterogeneity. Equation (6) quantifies the reduction of the hazard with respect to the level observed at the source, i.e., for an exposure concentration equal to C_0. The cumulative distribution function (CDF) and probability density function (PDF) of η are denoted by $P(\eta)$ and $f(\eta)$, respectively; in order to compute these functions we need to evaluate the travel time PDF $f(\tau)$.

Clearly, the distribution of η (6) depends on the joint PDF of τ and λ. While the generalization to random λ is straightforward, in the following we adopt for simplicity a deterministic λ (strictly applicable only in the case of radioactive decay). Hence, the CDF of the attenuation factor η is given by

$$P(\eta) = \int_{-\lambda^{-1}\ln\eta}^{\infty} f_\tau(\tau)d\tau = 1 - P_\tau\left(-\frac{\ln\eta}{\lambda}\right), \tag{7}$$

with f_τ and P_τ being the PDF and CDF of travel time τ, respectively. Consequently, the PDF of η is given by

$$f(\eta) = \frac{1}{\eta\lambda} f_\tau\left(-\frac{\ln\eta}{\lambda}\right). \tag{8}$$

3. Derivation of the Travel Time τ and Hazard Attenuation Factor η Distributions

Let the trajectory of a fluid (or nondiffusing tracer) particle originating at $t = 0$ at a point within A_0 of coordinates $\mathbf{b} = (b_y, b_z)$ be denoted by $\mathbf{x} = \mathbf{X}(t, \mathbf{b})$. The derivation of $\mathbf{X} = (X, Y, Z)$ from the assumed steady velocity field $\mathbf{V}(\mathbf{x})$ is achieved by integrating the kinematical differential equation

$$\frac{d\mathbf{X}}{dt} = \mathbf{V}(\mathbf{X}), \quad \text{with} \quad \mathbf{X}(0) = \mathbf{b}. \tag{9}$$

In numerical simulations, particle tracking is achieved by discretization of (9) and the computation of $f(\tau)$ is carried out by: (i) generating multiple realizations of the random *K*-field in the domain between the IP and CP; (ii) solving the flow equations (1) for conditions of mean constant head gradient *J* to obtain **V**; and (iii) subsequent integration of (9) to obtain **X** for a large number of points **b** in A_0. If A_0 is large enough to ensure

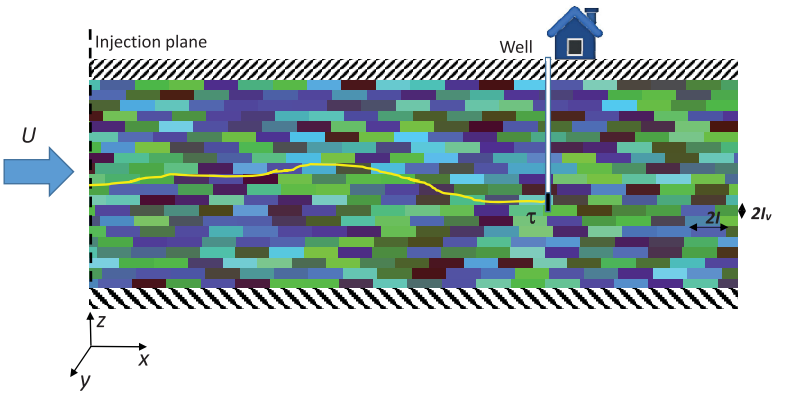

Figure 1. Illustration of the *Multi-Indicator Model* permeability structure used for solving the hydrodynamics by the *Self-consistent* approximation (SCA).

ergodicity, the PDF $f(\tau)$ can be identified from the single realization, otherwise a Monte Carlo procedure is the alternative. The travel time $\tau(x, \mathbf{b})$ is defined by $x = X(\tau, \mathbf{b})$, e.g., the time of first crossing of the CP.

The aforementioned numerical solution requires considerable computational resources (e.g. *Moslehi et al.* 2015) and it is generally not justified in view of the many other approximations. Two main methodologies have been pursued in the past in order to obtain approximate solutions. The first one is the first-order approximation in Y' (i.e., log-conductivity fluctuation), which leads to semianalytical expressions for the Inverse Gaussian $f(\tau)$ [*Shapiro and Cvetkovic*, 1988; *Dagan*, 1989] and are applicable to weakly heterogeneous formations (i.e., $\sigma_Y^2 < 1$). However, the aim of the paper is precisely to investigate the impact of high heterogeneity, encountered for instance at the MADE site. The second approximate approach we adopt herein for this purpose is the *Multi-Indicator Model* permeability structure and *Self-Consistent Approximation* (MIMSCA), whose essential steps are recapitulated briefly in the following.

MIMSCA has been developed over the past decade [*Dagan et al.*, 2003; *Jankovic et al.*, 2006] and its derivation is presented systematically in *Cvetkovic et al.* [2014]. The *Multi-Indicator Model* (MIM) structure is one of rectangular blocks (Figure 1) of sizes $2I$ in the horizontal plane and $2I_v$ in the z direction. They are of independent hydraulic conductivity of an univariate, known PDF $f(Y)$ such that the two-point auto-correlation is linear, e.g., $\rho(r_x, 0, 0) = 1 - r_x/(2I)$ for $0 < r_x < 2I$ and similarly in other directions. Thus, the structure is defined statistically and characterized entirely by $f(Y)$ and the integral scales I and I_v. If $f(Y)$ is a normal PDF, as adopted in this work, it is sufficient to characterize it through K_G and σ_Y^2. The numerical solution of flow and transport for such a structure is extremely demanding [e.g., *Jankovic et al.*, 2006, 2013] and an approximate semianalytical solution was obtained by SCA (the *Self-Consistent Approximation*). Thus, each block is surrounded by a homogeneous matrix of conductivity K_{ef} and after solving flow and transport, the solution for K_{ef}, the velocity and τ fields are obtained by superposition of the residuals associated with the ensemble of blocks. Further approximation implies that the travel time for streamlines crossing the block are constant and given by the one applying to the central streamline through a sphere of radius equal to I [see *Dagan et al.*, 2003, Figure 3]. The procedure leads to the following analytical expression of the travel time associated with a block of conductivity K:

$$\tau = x/U + \tau^* \quad \text{where} \quad \tau^*(\kappa) = \frac{2I}{3U}(1-\kappa)\left[\frac{2}{\kappa} + \frac{3}{2+\kappa}\,{}_2\mathcal{F}_1\left(\frac{2}{3}, 1, \frac{5}{3}, \frac{2(1-\kappa)}{(2+\kappa)}\right)\right], \tag{10}$$

with ${}_2\mathcal{F}_1$ is the hypergeometric function and $\kappa = K/K_{ef}$, while K_{ef}/K_G (which is a function of σ_Y^2) is determined by solving the following integral equation: $\int_{-\infty}^{\infty} (K/K_{ef} - 1)/(2 + K/K_{ef})\; f(Y)\, dY = 0$, with $Y = \ln(K/K_G)$ [*Dagan*, 1979]. The dependence of $\tau^* U/I$ upon $\ln(\kappa)$ [see *Cvetkovic et al.*, 2014, Figure 7 of the Supporting Information] is such that it decreases monotonously from infinity, for $\kappa \to 0$, proportional to $4/(3\kappa)$, to the constant $\tau^* U/I = -2.58$ for $\kappa \to \infty$. The strong asymmetry is the major feature of highly heterogeneous formations and is absent in the first order approximation which simplifies τ^* as a straight line near $\kappa = 1$.

MIMSCA provides the total travel time τ between the IP at $x=0$ and the CP at distance $x=2NI$, where N is an integer number of blocks as the BTC pertaining to flux proportional injection boundary condition as follows:

$$\mu(\tau,x)=\omega(\kappa_1)\ldots\omega(\kappa_N)\delta\left(\tau-x/U-\sum_{j=1}^{N}\tau_j^*\right), \tag{11}$$

where the travel times of the blocks, $\tau_j^*=\tau^*(\kappa_j)$, are statistically independent since the conductivities K_j are such. In the above expression $\omega=3\kappa/(2+\kappa)$ quantifies the effect of the different discharge conveyed by blocks of different κ which belong to the column of N blocks. It is seen that the process leading to τ is a time-domain random walk [*Cvetkovic et al.*, 2014].

Because τ_j^* (with $j=1,\ldots,N$) are statistically independent, the PDF of τ can be obtained by the N-fold convolution of the PDF of τ*. The latter is easily obtained as follows:

$$f(\tau^*)=-\omega(\xi(\tau^*))f_\kappa(\xi(\tau^*))\left(\frac{d\tau^*}{d\kappa}\right)^{-1}\Bigg|_{\kappa=\xi(\tau^*),}, \tag{12}$$

with f_κ representing the distribution of κ and $\kappa=\xi(\tau^*)$ is obtained by inverting the relationship $\tau^*(\kappa)$ (10) with $0\le\kappa\le\infty$. It is convenient to work in the Fourier space, for which the N-fold convolution of (12) writes

$$f_\tau(\tau;x)=\mathrm{FT}^{-1}\left[\tilde{f}(\tau_1^*)\cdot\tilde{f}(\tau_2^*)\ldots\tilde{f}(\tau_N^*)\right]=\mathrm{FT}^{-1}\left[\tilde{f}^N(\tau^*)\right], \tag{13}$$

where the tilde indicates Fourier Transform and FT^{-1} is its inverse and $N=x/(2I)$, which does not need to be an integer. Equation (13) applies because the travel times within the blocks are independent and identically distributed random variables. The resident injection condition, that is needed for the calculation of the travel time PDF (see section 2.1), is easily modeled along the approach of *Jankovic and Fiori* [2010] by imposing $\omega=1$ in (12) for the first segment $\tilde{f}(\tau_1^*)$ of the N-fold convolution (13). The calculations are efficiently performed by using Fast Fourier Transform, as function of the given f_κ. In the following we shall employ a lognormal distribution for κ.

4. Results and Discussion

We illustrate the methodology to investigate the impact of heterogeneity on the hazard attenuation factor η (6) associated with the concentration observed at a well characterized by a short screen. Although our main interest is highly heterogeneous aquifers, we shall explore a broad range of logconductivity variances σ_Y^2 to assess the impact of the spatial distribution of hydraulic conductivity on the distribution of η, the hazard attenuation factor. As previously discussed, see equation (6), η depends on the travel time distribution, which is calculated along the lines of section 3. Thus, we analyze first the CDF of τ (i.e., $P_\tau(\tau)$) as function of the distance x to the CP and the degree of heterogeneity σ_Y^2. For the sake of illustration we consider here two control planes at $x/I=4$ and 20, respectively, relatively close and far from the source. Results are computed for $\sigma_Y^2=$ 0.5, 1, 2, 4, and 8, with the latter value close to the one inferred at the MADE site [*Fiori et al.*, 2015b]. In this work we regard geological formations displaying $\sigma_Y^2>4$ to be highly heterogeneous. However, we point out that some studies report σ_Y^2 values to be larger than 20 for geological formations containing nonuniform hydrofacies with subhydrofacies-scale heterogeneity [see *Zhang et al.*, 2013, Table 1]. We also include, for the sake of reference, the CDF $P_\tau(\tau)=H(\tau-x/U)$ of τ for a homogeneous formation ($\sigma_Y^2=0$), where H is the Heaviside step function.

Table 1. List of Parameter Values Used in Figure 5

R_fD_ℓ	7×10^{-3} mg/(kg d)
R_fD_u	2.5×10^{-2} mg/(kg d)
IR/BW	3×10^{-2} l/(d kg)
AT	22550 days
ED	30 years
EF	350 days
C_0	3 mg/l

Figure 2 depicts the travel time CDF $P_\tau(\tau)$ for the different values of σ_Y^2, and for $x/I=4$ (Figure 2a) and $x/I=20$ (Figure 2b). Starting from the closest CP (Figure 2a) it is seen that $P_\tau(\tau)$ progressively departs from the CDF of a homogeneous formation (dashed line, $\tau=x/U$), displaying both an increasing density of fast arrivals ($\tau\le x/U$) and, most noteworthy, of travel times larger than x/U. The increase of the number of pathways characterized by such large values of τ becomes more

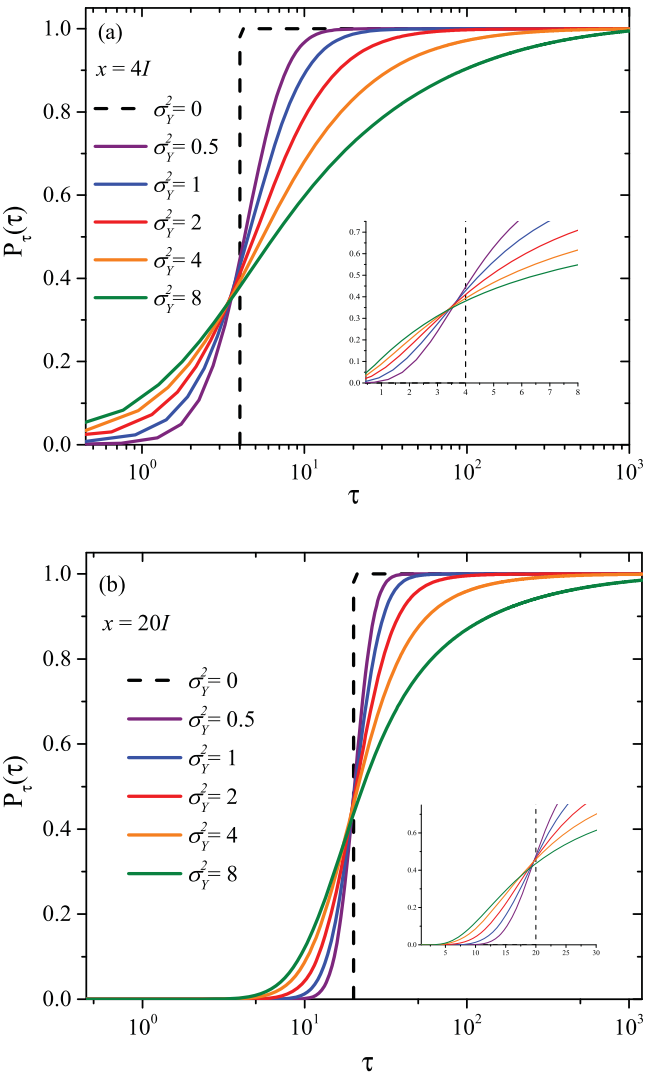

Figure 2. CDF of the travel time at a well with a small screen located at a distance of (a) $x = 4I$ and (b) $x = 20I$ from the source plane.

significant as σ_Y^2 increases. The deviations of P_τ from its homogeneous counterpart indicate two important effects of the spatial heterogeneity of K: (i) the emergence of "fast," preferential channels of the form of strings of blocks with large K, delivering solute at a velocity much larger than the mean U [*Wen and Gomez-Hernandez*, 1998; *Knudby and Carrera*, 2005; *Fiori and Jankovic*, 2012], and (ii) the presence of low-conductive zones, the density of which increases with σ_Y^2, in which the velocity is low and τ grows according to equation (10), leading to solute travel times to the well larger than x/U. The behavior displayed in Figure 2a indicates that the latter effect has a significant impact on the travel time CDF.

Similar considerations apply to $P_\tau(\tau)$ pertaining to larger distances from the source (Figure 2b, for $x = 20I$). As the distance between the source and the well increases, the likelihood of developing preferential channels of high velocity connecting the source to the well decreases, as there is a higher chance for a particle to encounter zones of low velocity along its path. As a consequence, the behavior of P_τ for $\tau \leq x/U$ is characterized by values closer to zero, manifesting a drop of the density of preferential "fast" channels with distance. Conversely, the low-velocity areas seem to dominate the travel time distribution for large σ_Y^2 at $x = 20I$ when compared to $x = 4I$ (see Figure 2a). Hence σ_Y^2, which encapsulates the degree of heterogeneity, has a large impact on the travel time distribution. This effect becomes noticeable for $\sigma_Y^2 > 0.5$. It is seen that the zones of low hydraulic conductivity play an important role. For lower heterogeneity, like at the Borden and Cape Cod sites [*Rajaram and Gelhar*, 1991; *LeBlanc et al.*, 1991], $P_\tau(\tau)$ is less affected by the low K zones.

The behavior of the CDF of τ governs the distribution of the hazard attenuation factor η, as it follows from the relation (7). We note that the parameter λ can assume different values as function of the particular process considered (anaerobic biodegradation, radioactive decay, or others). Even within the same process, e.g., anaerobic biodegradation, the parameter can vary according to several factors, like iron and manganese reduction and methanogenesis. For instance, *Zarlenga and Fiori* [2014] employed $\lambda I/U = 0.27$ for the modeling of core biodegradation at the Bemidji site [*Essaid et al.*, 2011]. For radioactive decay, the range of λ is larger (by several order of magnitudes) and depends on the particular isotope under consideration. For the sake of illustration we set in the following $\lambda I/U = 0.05$. Nevertheless, the impact of λ on $P(\tau)$ is straightforward and shall be analyzed later; it can be even made in a compact manner by introducing the new variable $-\lambda^{-1}\ln\eta$, which however may lead to a representation of the results less amenable to interpretation.

In Figure 3, we calculate $P(\eta)$ employing the same set of parameters used to generate Figures 2a and 2b, i.e., $\sigma_Y^2 =$ 0.5, 1, 2, 4, and 8 (solid lines with different colors), including the homogeneous case, i.e., $\sigma_Y^2 = 0$

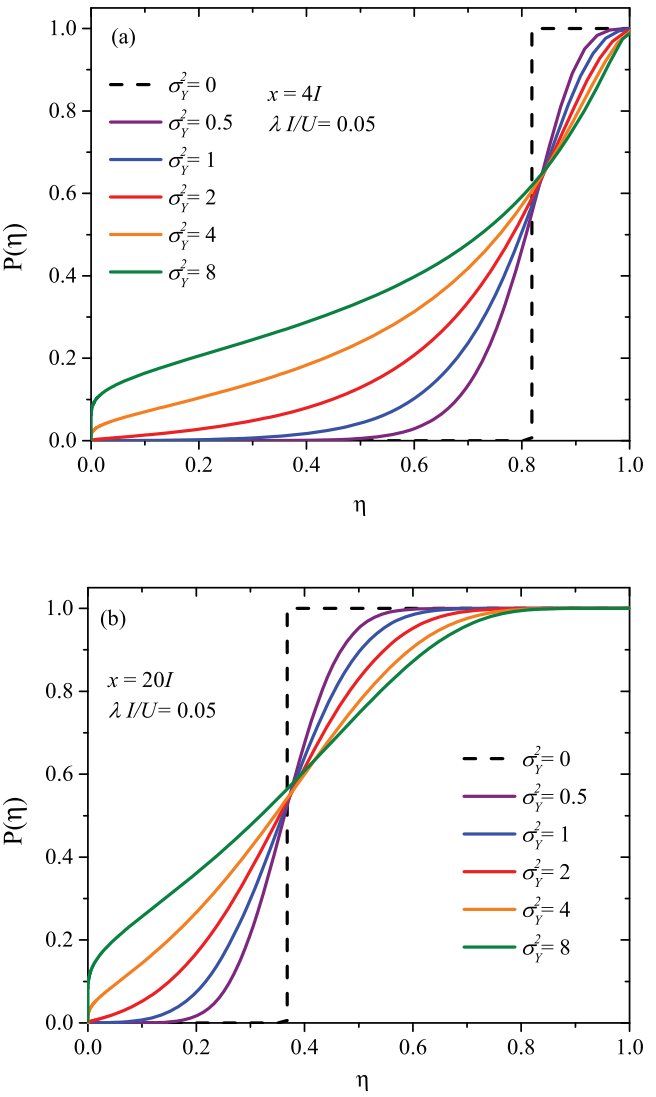

Figure 3. CDF of the hazard attenuation factor η at a well with a small screen located at a distance of (a) $x = 4I$ and (b) $x = 20I$ from the source plane. Results obtained for $\lambda I/U = 0.05$.

(dashed line), for $x/I = 4$ (Figure 3a) and $x/I = 20$ (Figure 3b), with $\lambda I/U = 0.05$. The CDF for the homogeneous case is simply given by $P(\eta) = H[\eta - \exp(-\lambda x/U)]$, where H is the Heaviside step function: there is no hazard until solute arrives at time $\tau = x/U$ with attenuation computed using the factor $\exp(-\lambda x/U)$ for $t > \tau$.

The curves show that $P(\eta)$ departs from the deterministic solution (dashed line) as heterogeneity increases, with the larger changes observed for low η. Figure 3 provides the probability that the hazard attenuation factor is lower than a given threshold, which can be computed as the ratio between the acceptable HI, for example according to toxicological studies or regulatory limits, and the value of HI_0 evaluated at the source by means of equation (3). Notice that larger values of η reflects a larger risk, since the concentration attenuation is smaller. Conversely, a smaller value of η means a smaller risk. In our work, η may assume any value from 0 to 1, with its occurrence encapsulated by $P(\eta)$. The behavior of $P(\eta)$ for large η is governed by the fast, preferential channels, characterized by small travel times, and hence, a modest reduction of the initial concentration C_0 (large η). Instead, a small η is obtained when the solute encounter blocks of low hydraulic conductivity, which increase the travel time to the well, causing a stronger reduction of C_0 (small η). Increasing levels of heterogeneity enhances the extent of such channels, leading to a broader distribution of η, with a larger probability to observe small values of η. The probability of exceeding a large η value increases with σ_Y^2 since higher heterogeneity facilitates the emergence of fast pathways with small travel times. However, higher σ_Y^2 values imply a larger occurrence of blocks of low hydraulic conductivity, which may trap the solute, thereby leading to larger probability of low η, with respect to a weakly heterogeneous formation (Figure 3a).

Increasing the distance between the source and the well leads to a shift of the curves toward the origin because of the expected increase, on average, of the travel times (Figure 3b). Otherwise, the behavior of the CDF of η is similar to the case of Figure 3a, as previously discussed.

Figure 4 displays the same cases of Figure 3, but with a larger $\lambda I/U = 0.1$. As expected, we observe a general shift of the curves toward $\eta = 0$ because of the stronger decay dictated by the larger λ, but the overall effect is similar to the one applying to the smaller λ (Figure 3).

Next, we illustrate the flexibility of the modeling framework to account for the uncertainty in human health related parameters. As shown in *Maxwell and Kastenberg* [1999] and *de Barros and Rubin* [2008], the uncertainty in human physiological response can affect the uncertainty in the overall risk. In general, when

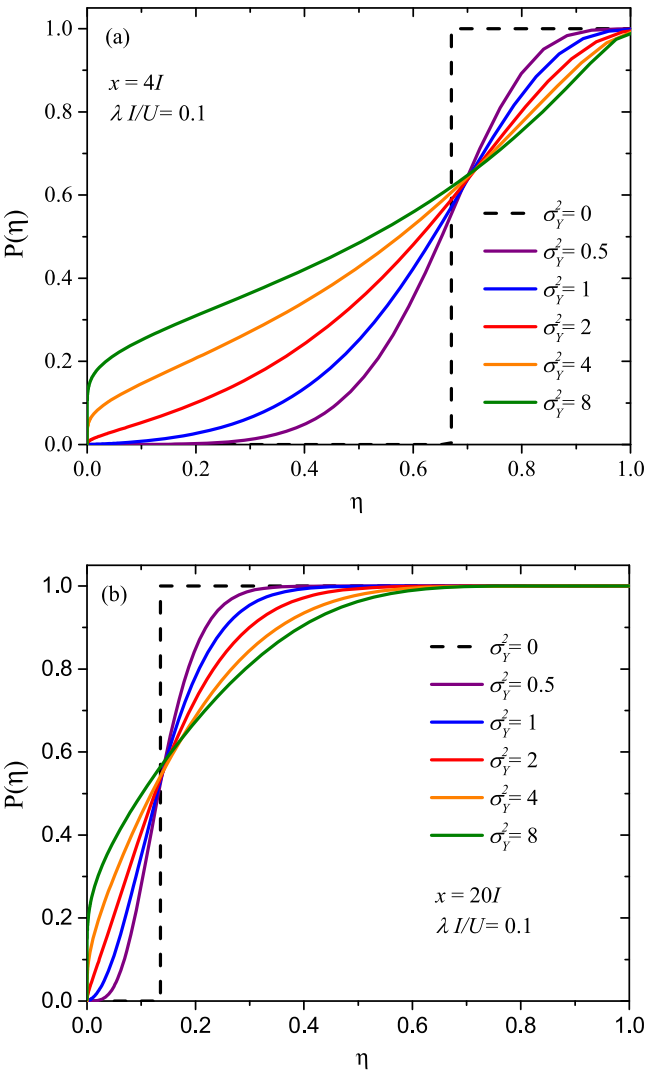

Figure 4. CDF of the hazard attenuation factor η at a well with a small screen located at a distance of (a) $x = 4I$ and (b) $x = 20I$ from the source plane. Results obtained for $\lambda I/U = 0.1$.

quantifying adverse human health effects, there are multiple sources of uncertainty which include the contaminant source history, hydrological parameters (e.g., the hydraulic conductivity), model conceptualization, human exposure, and physiological response among others [see *Andricevic and Cvetkovic*, 1996; *Maxwell et al*., 1999; *de Barros and Rubin*, 2008; *de Barros et al*., 2009; *Andricevic et al*., 2012; *Tartakovsky*, 2013]. Figure 5 depicts the CDF of the hazard index HI (3) for the case of a deterministic and uncertain reference dose R_fD. The CDF of HI was evaluated as follows:

$$P(\mathrm{HI}) = \int_0^\infty P(\mathrm{HI}|R_fD) f(R_fD) dR_fD, \quad (14)$$

where R_fD is characterized by its PDF $f(R_fD)$. The conditional CDF $P(\mathrm{HI}|R_fD)$ is computed using the same procedure used to obtain (7). The results shown in Figure 5 were evaluated assuming a uniform distribution for $f(R_fD)$. The uniform PDF is characterized by the lower and upper bounds of $f(R_fD)$, namely, R_fD_ℓ and R_fD_u. The parameters used to compute the results in Figure 5 are summarized in Table 1. Figure 5 shows the CDFs of HI for both a deterministic and uncertain R_fD. For this example, the CDF conditional on R_fD was computed using the mean value of R_fD. The case for low and high heterogeneity are displayed in Figure 5 at a longitudinal location of $x = 4I$. For this computational illustration, the uncertainty in R_fD becomes noticeable for $\mathrm{HI} > 1$ for both $\sigma_Y^2 = 1$ and 8. In the case of $\sigma_Y^2 = 8$, the probability of $\mathrm{HI} < 1$ is approximately equal to 0.65 while for $\sigma_Y^2 = 1$, the probability value is estimated to be around 0.25. The probability of $\mathrm{HI} < 1$ is larger for the case $\sigma_Y^2 = 8$ (as opposed to $\sigma_Y^2 = 1$) since larger heterogeneity implies the occurrence of low conductivity zones which can trap the contaminant thus increasing the probability of low values of HI. Similar analysis can be performed by considering the uncertainty stemming from other parameters listed in Table 1.

5. Summary and Conclusions

In the present work we discuss the combined effect of contaminant decay rate and subsurface formation heterogeneity on the noncarcinogenic risk uncertainty at a production well. The analysis is conducted under the simplifying assumptions that solute reactivity can be represented through a contaminant decay rate λ and that the travel time of the solute particle can be computed by neglecting the effect of convergent radial flow close to the production well. The latter assumption implies that once the particle enters the capture zone of the well, it continues to travel with the same velocity that it would experience under natural flow conditions.

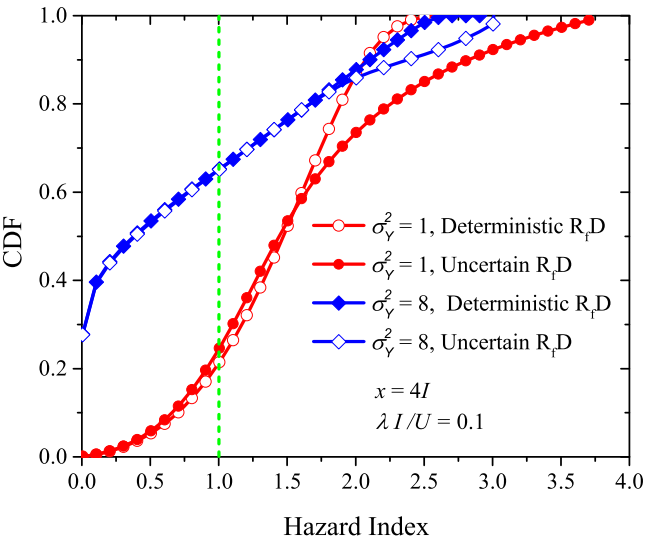

Figure 5. CDF of the hazard index HI at a well with a small screen located at a distance of $x = 4I$ from the injection zone. Results for $\sigma_Y^2 = 1$ and $\sigma_Y^2 = 8$. The results presented were obtained for $\lambda I/U = 0.1$ and the parameters listed in Table 1.

In the present study we analyzed the hazard attenuation factor η, see equation (6), defined as the ratio between the hazard indices at the well and at the source. Due to the spatial variability of permeability, η is a random variable, fully characterized by its CDF. We analyzed the CDF of the hazard attenuation factor for a well of a small screen intercepting a plume traveling in a heterogeneous formation for σ_Y^2 ranging from 0 (homogeneous formation) to 8 and a contaminant decay rate λ, under conditions of three-dimensional steady natural gradient flow. Heterogeneity is modeled in a three-dimensional setup by using the MIM structure and SCA of flow and transport, which is formally valid for any degree of heterogeneity.

The main conclusions of the analysis are that for a given λ, aquifer heterogeneity has a strong impact on the CDF of η. The main effect of heterogeneity is the reduction (in a probabilistic sense) of the hazard relative to a homogeneous formation due to the presence of zones of low conductivity on the plume path which cause a considerable increase of the travel time and consequently a larger decay. This important effect, amplified by large σ_Y^2, is associated with later arrival of the plume at the pumping well. Therefore our work quantifies the significance of these low-conductive zones in augmenting the probability of lower risks, This effect is not so pronounced in geological formations displaying $\sigma_Y^2 < 1$. The opposite effect, of larger hazard at travel times smaller than the mean x/U, is also significant.

It is emphasized that the particular case selected in order to illustrate the impact of large σ_Y^2, as encountered at the MADE site, is an extreme one. Though diffusive and local-scale dispersion may play a role in many circumstances, its impact in the present case is negligible due to the high Peclet number encountered in applications and the overriding effect of decay. Similarly, for larger capture zones, pertinent to a well of higher discharge or to a battery of wells, the solute arrives along an ensemble of streamtubes, rather than along a thin one as considered here. A larger capture zone averages travel times and attenuation factors thereby reducing uncertainty [e.g., *de Barros et al.*, 2009]. The impact of the increase of the capture zone upon hazard attenuation factor is the object of a future study. Finally, we also highlight that the effects of geological stratification can affect the risk estimation. The works of *Siirila and Maxwell* [2012] and *de Barros and Fiori* [2014] showed numerically and analytically how the statistical anisotropy in the correlation scales of the conductivity field can influence the uncertainty in risk for a given range of heterogeneity. A systematic investigation on the interplay between stratification and heterogeneity is also subject of future research.

Acknowledgments
The second author (AB) was supported by the European Communities 7th Framework Programme under grant agreement no. 603629-ENV-2013-6.2.1-Globaqua. Partial support for the third author (V.C.) was provided by the Swedish Nuclear Fuel and Waste Management Co (SKB). There are no data sharing issues since all of the numerical information is provided in the figures produced by solving the equations in the paper.

References

Andricevic, R., and V. Cvetkovic (1996), Evaluation of risk from contaminants migrating by groundwater, *Water Resour. Res.*, *32*(3), 611–621.
Andricevic, R., V. Srzic, and H. Gotovac (2012), Risk characterization for toxic chemicals transported in aquifers, *Adv. Water Resour.*, *36*, 86–97.
Andrivevic, R., J. I. Daniels, and R. L. Jacobson (1994), Radionuclide migration using a travel time transport approach and its application in risk analysis, *J. Hydrol.*, *163*(1–2), 125–145.
Atchley, A. L., R. M. Maxwell, and A. K. Navarre-Sitchler (2013), Human health risk assessment of CO_2 leakage into overlying aquifers using a stochastic, geochemical reactive transport approach, *Environ. Sci. Technol.*, *47*(11), 5954–5962.
Benekos, I., C. Shoemaker, and J. Stedinger (2007), Probabilistic risk and uncertainty analysis for bioremediation of four chlorinated ethenes in groundwater, *Stochastic Environ. Res. Risk Assess.*, *21*(4), 375–390.
Beyer, C., S. Altfelder, W. H. Duijnisveld, and T. Streck (2009), Modelling spatial variability and uncertainty of cadmium leaching to groundwater in an urban region, *J. Hydrol.*, *369*(3), 274–283.
Bogen, K. T., and R. C. Spear (1987), Integrating uncertainty and interindividual variability in environmental risk assessment, *Risk Analysis*, *7*(4), 427–436.

Bohling, G. C., G. Liu, S. J. Knobbe, E. C. Reboulet, D. W. Hyndman, P. Dietrich, and J. J. Butler (2012), Geostatistical analysis of centimeter-scale hydraulic conductivity variations at the made site, *Water Resour. Res.*, *48*, W02525, doi:10.1029/2011WR010791.
Cvetkovic, V. (2011), Tracer attenuation in groundwater, *Water Resour. Res.*, *47*, W12541, doi:10.1029/2011WR010999.
Cvetkovic, V., and S. Molin (2012), Combining numerical simulations with time-domain random walk for pathogen risk assessment in groundwater, *Adv. Water Resour.*, *36*, 98–107.
Cvetkovic, V., A. Fiori, and G. Dagan (2014), Solute transport in aquifers of arbitrary variability: A time-domain random walk formulation, *Water Resour. Res.*, *50*, 5759–5773, doi:10.1002/2014WR015449.
Dagan, G. (1979), Models of groundwater flow in statistically homogeneous porous formations, *Water Resour. Res.*, *15*(1), 47–63.
Dagan, G. (1989), *Flow and Transport in Porous Formations*, Springer, Berlin Heidelberg, doi:10.1007/978-3-642-75015-1.
Dagan, G., A. Fiori, and I. Janković (2003), Flow and transport in highly heterogeneous formations: 1. Conceptual framework and validity of first-order approximations, *Water Resour. Res.*, *39*(9), 1268, doi:10.1029/2002WR001717.
de Barros, F. P. J., and A. Fiori (2014), First-order based cumulative distribution function for solute concentration in heterogeneous aquifers: Theoretical analysis and implications for human health risk assessment, *Water Resour. Res.*, *50*, 4018–4037, doi:10.1002/2013WR015024.
de Barros, F. P. J., and Y. Rubin (2008), A risk-driven approach for subsurface site characterization, *Water Resour. Res.*, *44*, W01414, doi:10.1029/2007WR006081.
de Barros, F. P. J., Y. Rubin, and R. M. Maxwell (2009), The concept of comparative information yield curves and its application to risk-based site characterization, *Water Resour. Res.*, *45*, W06401, doi:10.1029/2008WR007324.
de Barros, F. P. J., S. Ezzedine, and Y. Rubin (2012), Impact of hydrogeological data on measures of uncertainty, site characterization and environmental performance metrics, *Adv. Water Resour.*, *36*, 51–63.
Dogan, M., R. L. Van Dam, G. Liu, M. M. Meerschaert, J. J. Butler, G. C. Bohling, D. A. Benson, and D. W. Hyndman (2014), Predicting flow and transport in highly heterogeneous alluvial aquifers, *Geophys. Res. Lett.*, *41*, 7560–7565, doi:10.1002/2014GL061800.
Essaid, H. I., B. A. Bekins, W. N. Herkelrath, and G. N. Delin (2011), Crude oil at the bemidji site: 25 years of monitoring, modeling, and understanding, *Ground Water*, *49*(5), 706–726.
Fiori, A., and I. Jankovic (2012), On preferential flow, channeling and connectivity in heterogeneous porous formations, *Math. Geosci.*, *44*(2), 133–145.
Fiori, A., G. Dagan, I. Jankovic, and A. Zarlenga (2013), The plume spreading in the made transport experiment: Could it be predicted by stochastic models?, *Water Resour. Res.*, *49*, 2497–2507, doi:10.1002/wrcr.20128.
Fiori, A., A. Bellin, V. Cvetkovic, F. P. J. de Barros, and G. Dagan (2015a), Stochastic modeling of solute transport in aquifers: From heterogeneity characterization to risk analysis, *Water Resour. Res.*, *51*, 6622–6648, doi:10.1002/2015WR017388.
Fiori, A., E. Volpi, A. Zarlenga, and G. C. Bohling (2015b), Gaussian or non-Gaussian logconductivity distribution at the made site: What is its impact on the breakthrough curve?, *J. Contam. Hydrol.*, *179*, 25–34.
Fjeld, R. A., N. A. Eisenberg, and K. L. Compton (2007), *Quantitative Environmental Risk Analysis for Human Health*, John Wiley & Sons, N. J.
Gomez-Hernandez, J., J. J. Butler, and A. Fiori (2016), Groundwater transport in highly heterogeneous aquifers, *Eos*, *97*, doi:10.1029/2016EO047263.
Harvey, C., and S. M. Gorelick (2000), Rate-limited mass transfer or macrodispersion: Which dominates plume evolution at the macrodispersion experiment made site?, *Water Resour. Res.*, *36*(3), 637–650.
Henri, C. V., D. Fernandez-Garcia, and F. P. J. de Barros (2015), Probabilistic human health risk assessment of degradation-related chemical mixtures in heterogeneous aquifers: Risk statistics, hot spots, and preferential channels, *Water Resour. Res.*, *51*, 4086–4108, doi:10.1002/2014WR016717.
Henri, C. V., D. Fernandez-Garcia, and F. P. J. de Barros (2016), Assessing the joint impact of DNAPL source-zone behavior and degradation products on the probabilistic characterization of human health risk, *Adv. Water Resour.*, *88*, 124–138.
Jankovic, I., and A. Fiori (2010), Analysis of the impact of injection mode in transport through strongly heterogeneous aquifers, *Adv. Water Resour.*, *33*(10), 1199–1205, doi:10.1016/j.advwatres.2010.05.006.
Jankovic, I., A. Fiori, and G. Dagan (2006), Modeling flow and transport in highly heterogeneous three-dimensional aquifers: Ergodicity, Gaussianity, and anomalous behavior: 1. Conceptual issues and numerical simulations, *Water Resour. Res.*, *42*, W06D12, doi:10.1029/2005WR004734.
Jankovic, I., A. Fiori, and G. Dagan (2013), Effective conductivity of isotropic highly heterogeneous formations: Numerical and theoretical issues, *Water Resour. Res.*, *49*, 1178–1183, doi:10.1029/2012WR012441.
Knudby, C., and J. Carrera (2005), On the relationship between indicators of geostatistical, flow and transport connectivity, *Adv. Water Resour.*, *28*(4), 405–421.
LeBlanc, D. R., S. P. Garabedian, K. M. Hess, L. W. Gelhar, R. D. Quadri, K. G. Stollenwerk, and W. W. Wood (1991), Large-scale natural gradient tracer test in sand and gravel, Cape Cod, Massachusetts: 1. Experimental design and observed tracer movement, *Water Resour. Res.*, *27*(5), 895–910, doi:10.1029/91WR00241.
Maxwell, R. M., and W. E. Kastenberg (1999), Stochastic environmental risk analysis: An integrated methodology for predicting cancer risk from contaminated groundwater, *Stochastic Environ. Res. Risk Assess.*, *13*(1–2), 27–47.
Maxwell, R. M., W. E. Kastenberg, and Y. Rubin (1999), A methodology to integrate site characterization information into groundwater-driven health risk assessment, *Water Resour. Res.*, *35*(9), 2841–2855.
Molin, S., and V. Cvetkovic (2010), Microbial risk assessment in heterogeneous aquifers: 1. Pathogen transport, *Water Resour. Res.*, *46*, W05518, doi:10.1029/2009WR008036.
Molin, S., V. Cvetkovic, and T. Stenstrom (2010), Microbial risk assessment in heterogeneous aquifers: 2. Infection risk sensitivity, *Water Resour. Res.*, *46*, W05519, doi:10.1029/2009WR008039.
Moslehi, M., R. Rajagopal, and F. P. J. de Barros (2015), Optimal allocation of computational resources in hydrogeological models under uncertainty, *Advanc. Water Res.*, *83*, 299–309, doi:10.1016/j.advwatres.2015.06.014.
Rajaram, H., and L. W. Gelhar (1991), Three-dimensional spatial moments analysis of the Borden tracer test, *Water Resour. Res.*, *27*(6), 1239–1251.
Rodak, C., and S. Silliman (2012), Probabilistic risk analysis and fault trees: Initial discussion of application to identification of risk at a well-head, *Adv. Water Resour.*, *36*, 133–145.
Rubin, Y. (2003), *Applied Stochastic Hydrology*, Oxford Univ. Press, Oxford, U. K.
Rubin, Y., M. Cushey, and A. Bellin (1994), Modeling of transport in groundwater for environmental risk assessment, *Stochastic Hydrol. Hydraul.*, *8*(1), 57–77.
Salamon, P., D. Fernandez-Garcia, and J. Gomez-Hernandez (2007), Modeling tracer transport at the made site: The importance of heterogeneity, *Water Resour. Res.*, *43*, W08404, doi:10.1029/2006WR005522.

Shapiro, A. M., and V. D. Cvetkovic (1988), Stochastic analysis of solute arrival time in heterogeneous porous media, *Water Resour. Res.*, *24*(10), 1711–1718.
Siirila, E. R., and R. M. Maxwell (2012), Evaluating effective reaction rates of kinetically driven solutes in large-scale, statistically anisotropic media: Human health risk implications, *Water Resour. Res.*, *48*, W04527, doi:10.1029/2011WR011516.
Siirila, E. R., A. K. Navarre-Sitchler, R. M. Maxwell, and J. E. McCray (2012), A quantitative methodology to assess the risks to human health from CO_2 leakage into groundwater, *Adv. Water Resour.*, *36*, 146–164.
Tartakovsky, D. M. (2007), Probabilistic risk analysis in subsurface hydrology, *Geophys. Res. Lett.*, *34*, L05404, doi:10.1029/2007GL029245.
Tartakovsky, D. M. (2013), Assessment and management of risk in subsurface hydrology: A review and perspective, *Adv. Water Resour.*, *51*, 247–260.
USEPA (1989), Risk assessment guidance for superfund: Human health manual (Part A), *Tech. Rep. EPA/540/189/002*, vol. 1, Washington, D. C.
Wen, X.-H., and J. J. Gomez-Hernandez (1998), Numerical modeling of macrodispersion in heterogeneous media: a comparison of multi-Gaussian and non-multi-Gaussian models, *J. Contam. Hydrol.*, *30*(1), 129–156.
Yu, W. H., C. M. Harvey, and C. F. Harvey (2003), Arsenic in groundwater in Bangladesh: A geostatistical and epidemiological framework for evaluating health effects and potential remedies, *Water Resour. Res.*, *39*(6), 1146, doi:10.1029/2002WR001327.
Zarlenga, A., and A. Fiori (2014), Stochastic analytical modeling of the biodegradation of steady plumes, *J. Contam. Hydrol.*, *157*, 106–116.
Zhang, Y., C. T. Green, and G. E. Fogg (2013), The impact of medium architecture of alluvial settings on non-Fickian transport, *Adv. Water Resour.*, *54*, 78–99.
Zheng, C., M. Bianchi, and S. M. Gorelick (2011), Lessons learned from 25 years of research at the made site, *Ground Water*, *49*(5), 649–662.